Physica Status Solidi (RRL) - Rapid Research Letters

Highly-efficient superstrate Cu2ZnSnS4 solar cell fabricated by low-cost methods

--Manuscript Draft--

Manuscript Number:	pssr.201700144
Full Title:	Highly-efficient superstrate Cu2ZnSnS4 solar cell fabricated by low-cost methods
Article Type:	Rapid Research Letter
Section/Category:	Solar cells and photovoltaics
Keywords:	semiconductors; CZTS; electrodeposition; superstrate solar cell
Corresponding Author:	Yesica Di Iorio, PhD INTEMA-CONICET ARGENTINA
Additional Information:	
Question	**Response**
Please submit a plain text version of your cover letter here. Please note, if you are submitting a revision of your manuscript, there is an opportunity for you to provide your responses to the reviewers later; please do not add them to the cover letter.	Mar del Plata, May 11, 2017 Stefan Hildebrandt Editor-in-chief Physica Status Solidi (RRL) Please find enclosed the manuscript “Highly-efficient superstrate Cu2ZnSnS4 solar cell fabricated by low cost methods” by M. Berruet, Y. Di Iorio, C. J. Pereyra, R.E. Marotti, M. Vázquez. I would greatly appreciate if you would consider it for publication in Physica Status Solidi (RRL). The article is original, unpublished and not being considered for publication elsewhere. In this manuscript, we describe the preparation of a highly efficiency thin film solar cell in superstrate configuration composed by FTO/TiO2/In2S3/Cu2ZnSnS4/graphite is reported. A maximum conversion efficiency of 3.5 % has been achieved for the first time using this configuration and materials. The device was prepared by low cost methods without toxic components. Supporting Information was added. I thank you in advance. Sincerely, Dr. Yesica Di Iorio
Do you or any of your co-authors have a conflict of interest to declare?	No. The authors declare no conflict of interest.
Corresponding Author Secondary Information:	
Corresponding Author's Institution:	INTEMA-CONICET
Corresponding Author's Secondary Institution:	
First Author:	Mariana Berruet
First Author Secondary Information:	
Order of Authors:	Mariana Berruet
	Yesica Di Iorio, PhD
	Javier Pereyra
	Ricardo Marotti
	Marcela Vazquez

Order of Authors Secondary Information:	
Abstract:	A recent accomplishment in the preparation of a highly efficient thin film solar cell is reported. This superstrate cell is composed by FTO/TiO2/In2S3/Cu2ZnSnS4/graphite. A maximum conversion efficiency of 3.5 % has been achieved for the first time using this configuration and materials. The device includes low cost methods and non-toxic components. Details of the experimental procedures are provided and the device characterization data are presented and analyzed.

pss-Header will be provided by the publisher

Highly-efficient superstrate Cu_2ZnSnS_4 solar cell fabricated by low-cost methods

M. Berruet[1], Y. Di Iorio[*,1] C. J. Pereyra[2], R.E. Marotti[2], M. Vázquez[1]

[1] División Electroquímica Aplicada, INTEMA, Facultad de Ingeniería, CONICET-Universidad Nacional de Mar del Plata, J.B. Justo 4302, B7608FDQ Mar del Plata, Argentina
[2] Instituto de Física and CINQUIFIMA, Facultad de Ingeniería, Universidad de la República, Julio Herrera y Reissig 565, C.C. 30, 11000 Montevideo, Uruguay

Received ZZZ, revised ZZZ, accepted ZZZ
Published online ZZZ(Dates will be provided by the publisher.)

Keywords semiconductors; CZTS; electrodeposition; superstrate solar cell.

* Corresponding author: yesica.diiorio@fi.mdp.edu.ar, Phone: +54 223 481 6600

A recent accomplishment in the preparation of a highly efficient thin film solar cell is reported. This superstrate cell is composed by FTO/TiO_2/In_2S_3/Cu_2ZnSnS_4/graphite. A maximum conversion efficiency of 3.5 % has been achieved for the first time using this configuration and materials. The device includes low cost methods and non-toxic components. Details of the experimental procedures are provided and the device characterization data are presented and analyzed.

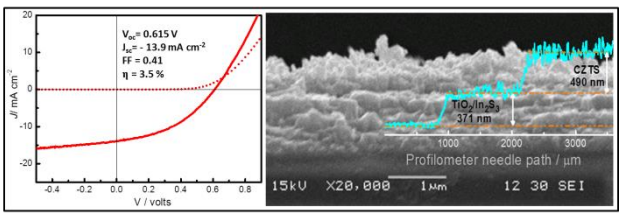

Left: Current-voltage response of the best cell FTO/TiO_2/In_2S_3/Cu_2ZnSnS_4/graphite in the dark (dotted line) and under simulated solar irradiation (solid line). Right: Cross-sectional view of the cell. Inset: Profilometric scan of the device.

1 Introduction Due to the scarcity and high cost of indium and gallium [1], kesterite Cu_2ZnSnS_4 (CZTS) has attracted research interest as an alternative material to replace chalcopyrite $Cu(In,Ga)S_2$ (CIGS) in thin-film photovoltaic cells. Although optical properties such as the direct bandgap and absorption coefficient of these two materials are similar, the efficiencies reported so far for CZTS solar cells are much lower. This has mainly been attributed to stannite inclusions or to several non-ideal recombination channels: (i) recombination at the interface between kesterite and the buffer layer and (ii) a recombination process due to a very high density of defects, comparable to the density of states in the band [2]. Moreover, non-stoichiometric phases such as SnS and poor grain formation can be translated into a low mobility and lifetime of carriers, resulting in a low quality CZTS thin film [2, 3].

The Shockley Queisser detailed balances hypothesis yields a theoretical efficiency for single junction kesterite CZTS of 32.4% [4]. Although this is an unrealistic limit, it can be used to estimate the role of different loss mechanisms. It has been reported that the more severe losses are associated to dominant interface recombination, high series resistance and low minority carrier lifetime [5]. Since the first reported sulfide CZTS solar cell in 1996, and according to our knowledge, the record efficiencies in substrate configuration have evolved from 0.66 to 8.8 % in 2015 [6]. However, if only non-vacuum CZTS deposition routes are taken into account, the highest efficiencies drop to 3.4 % for cells obtained by electrodeposition and 1.61 % for ink sol gel combined approaches [7, 8]. In superstrate configuration, the evolution is rather different and even if the efficiencies are lower, they are still interesting concept proofs for applications such as tandem or flexible cells. Ghosh *et al.* have reported a conversion efficiency of

3.63% for ITO/ZnONR/ZnS/CZTS/Au combining hydrothermal, chemical bath deposition and spin coating assisted ink routes [9]. Chen *et al.* have achieved an efficiency of 0.6 % using a screen printing technique for carbon paste/CZTS/In_2S_3/TiO_2NP/FTO [10].

This short communication reports the successful preparation of a thin CZTS superestrate solar cell (FTO/TiO_2/In_2S_3/Cu_2ZnSnS_4/graphite) with a maximum efficiency of 3.53% at lab-scale. The solar cell has been designed using a novel production process in which the absorber, the buffer and the window layers are all deposited using solution-base tecniques, as well as eco-friendly and low-cost processes that involve non-toxic materials and avoid vacuum, Cd containing layers and purification or selenization stages.

2 Experimental details

2.1 Device structure The cells were prepared in superstrate configuration using FTO (SnO_2:F, Zhuhai Kaivo Electronic Components Co., Ltd.) as substrate.

The substrates (2 x 2 cm^2) were coated with a thin layer of TiO_2 (300 nm) and an ultrathin layer of In_2S_3 (60 nm) deposited by spray pyrolysis as previously reported [11, 12]. Then, Cu_2ZnSnS_4 films (500 nm) were electrodeposited on top of them using a typical three-electrode cell with FTO, saturated calomel electrode (SCE) and Pt mesh as working, reference and counter electrodes, respectively. The FTO active area was defined by a circular mask of 1.22 cm^2.

The electrolytic bath was prepared following the procedure of Pawar *et al.* [13]. The films were deposited applying a fixed potential (E = -1.05 V vs SCE) during 15 minutes at room temperature with a slowly stirring using as potentiostat a Solartron Instrument 1280B. Then, the films were annealed in sulfur vapor atmosphere (sulfur powder) at 580º C for 90 minutes using a purpose built reactor [14]. The morphological and structural characterization of CZTS films onto FTO/TiO_2/In_2S_3 are presented as supporting information (Figs S1 and S2).

To complete the cell, twelve graphite dots of 0.023 cm^2 (effective area of the solar cell) were painted with conductive graphite inks using a mask on each sample (Alpha Aesar) and used as back contacts.

2.2 Characterization The thickness of each layer was evaluated using a KLA TENCOR D-100 profilometer and corroborated with cross section SEM images using a JEOL JSM-6460LV microscope as shown in the graphical abstract. Current–voltage curves were recorded using an IVIUM® compact potentiostat under 100 mW cm^{-2} (1 Sun) irradiance. The light source was a 150 W Xe lamp coupled to an air-mass filter 1.5G (solar simulator, Oriel-Newport 69907). The light intensity was calibrated with a Si photodiode.

In order to study the internal charge carrier dynamics of the solar cells, Intensity Modulated Photovoltage and Photocurrent Spectroscopy (IMVS & IMPS respectively) were evaluated. For the optical excitation a modulated red LED (639 nm, ~ 1 mW) was used and various frequency sweeps were performed from 2 Hz to 100 kHz. The photovoltage and photocurrent modulated amplitudes and phases ($I_{IMVS,IMPS}$ (ω)) were detected by two lock-in amplifiers (Stanford Research Systems SRS-530). Finally a photodiode (UV Enhanced Silicon Detector) was used to monitor the LED signal. The LED modulated signal was driven by a signal generator (Tecktronix AFG 3022B).

For the photoresponse measurement (PR) a 50 W halogen lamp (Newport 6337) was used as a source of white light excitation, which was monochromatized (ORIEL 77250) and chopped (SR 540) before reaching the sample. The chopping frequency was smaller than the one obtained from IMPS characteristic frequency. The current signal (in short circuit condition) was detected by a lock-in amplifier (SRS SR530). For the reference signal, the experimental setup was calibrated by means of an Ocean Optics S2000 spectrometer and an Oriel 70260 Power Meter.

3 Results and discussion

The current- voltage curves of the best cell in the dark and under illumination are shown in Figure 1. Table 1 summarizes the main solar cell parameters, such as short circuit density current (J_{sc}), open circuit voltage (V_{oc}), fill factor (FF) and solar conversion efficiency (η). Internal parameters such as series and shunt resistances under illumination ($R_{s,L}$, $R_{sh,L}$) ideality factor (n) and reverse saturation current density (J_0) are calculated from V_{oc}-J_{sc} measurements assuming a single diode model and varying the incident illumination intensity [15] (see supporting information, Fig S3).

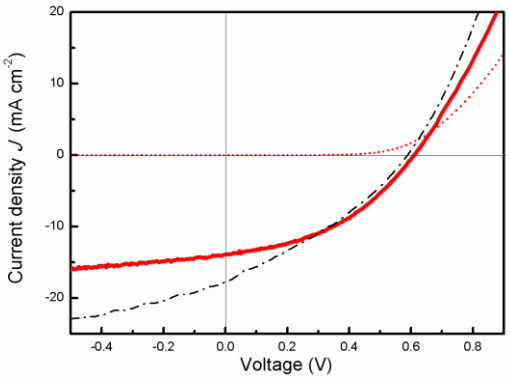

Figure 1 Current-voltage response of the best cell FTO/TiO_2/In_2S_3/Cu_2ZnSnS_4/graphite in the dark (dotted line) and under solar irradiation (solid line). The black dash dotted line corresponds to a similar solar cell, but with CIS as absorber.

The CZTS device shows an improvement in the values of V_{oc}, J_{sc} and FF, as well as efficiency compared to previous reported works with TiO_2 and In_2S_3 as n-type

semiconductors [10, 16-18]. J_{sc} is even higher than that in the nanostructured solar cell reported by Ghosh *et al.* [9], where J_{sc}=8.5 mA cm^{-2} was achieved for the maximum efficiency reported in superstrate configuration. However, due to the extensive amount of variables (e.g. architecture, materials and experimental procedures), it is not easy to understand and identify the electrical and optical loss mechanisms just by comparing the performance between solar cells fabricated by different authors.

Table 1: Relevant electrical parameters for the solar cells presented in Figure 1: FTO/TiO_2/In_2S_3/Cu_2ZnSnS_4/graphite and FTO/TiO_2/In_2S_3/$CuInS_2$/graphite.

	CZTS solar cell	*CIS solar cell*
J_{SC} / mA cm^{-2}	**13.9**	**17.7**[*]
V_{OC} / V	**0.615**	**0.583**[*]
FF	**0.41**	**0.32**[*]
η %	**3.53**	**3.3**[*]
R_s / Ωcm^2	**5.9**	**2.4**
R_{sh} / Ωcm^2	**151**	**45.6**
n	**1.78**	**0.8**
J_0/ A cm^{-2}	**2.9 10^{-8}**	**1.4 10^{-7}**
τ_R / ms	**0.6**	**0.13**
τ_D / ms	**0.05**	**0.05**
η_{cc} %	**92**	**62**

[*]Previously reported [14]

For these reasons, a $CuInS_2$ (CIS) solar cell fabricated using identical procedures than those in the CZTS solar cell has been included in Fig 1 and Table 1 for comparison [14]. The thickness (d) of both absorber layers are similar and less than 500 nm. In several publications, the J_{sc} is found to decrease when d< 1 μm [19, 20]. This can be explained by the average absorption length of band edge photons (1/α). Nevertheless, the limiting absorber thickness strongly depends on recombination rate and reflections in the back contact [21, 22]. Moreover, if the absorber thickness is reduced, the width of the recombination zone can be reduced, thus increasing V_{oc} [21]. Such is the present case, where the thickness minimal (d ≈ 500 nm); but still the photocurrent generation is high, and the deficit V_{oc} (V_{oc}q -E_g) is minimum resigning optical losses due to incomplete light absorption. The fact that a very thin absorbing layer translates into a higher V_{oc} is a consequence of the imperfect bulk quality of the CZTS including small grain size, grain boundaries as recombination centres and a high density of shunt paths.

The J_0 of the CZTS cell is one order of magnitude lower than that of CIS indicating less influence of the recombination mechanism (see Table 1).

The electrical parameters (J_{sc} and V_{oc}) are comparable for both cells but mainly the FF is lower for the CIS device due to the smaller R_{sh} value as can be seen from Table 1 and the curvature of curves under illumination in Fig.1.

IMVS and IMPS techniques are closely related to the inner dynamics of the charge carriers, specifically with the charge recombination dynamics in the bulk semiconductor and at the interfaces [23-25]. As IMVS is measured at open-circuit it is possible to explore the electron lifetime and electron-hole recombination dynamics, as in this condition the excited electron-hole pair can only return to the equilibrium condition by recombination [26]. With IMPS (at short circuit conditions), it is possible to obtain information about the combined effect of the charge carriers mass transport and recombination. If the charge collection process is faster than the recombination process, then the IMPS signal would lead to the characteristic time constant of the transport process. So, the charge recombination at open circuit (τ_R) and the charge collection at short circuit (τ_D) can be obtained from the frequency minima of the imaginary component in the IMVS and IMPS response, respectively. Then, a rough estimation of charge collection efficiency (η_{cc}) can be calculated as $\eta_{cc} = 1 - \tau_D/\tau_R$ to appraise how good the collection of charge carriers within the cell is [26, 27]. The characteristic IMVS curves are shown in the supporting information (Figs. S4 and S5) and the relevant parameters are summarized in Table 1. It can be seen that while the mass transport times from both cells are identical, the recombination time of the photogenerated carriers is almost five times higher for the CZTS cell, producing a clear improvement in the charge collection efficiency η_{cc}, which is reflected again in the best FF. Accordingly, the improvement in the FF value could be attributed to better charge transport and collection in the CZTS device.

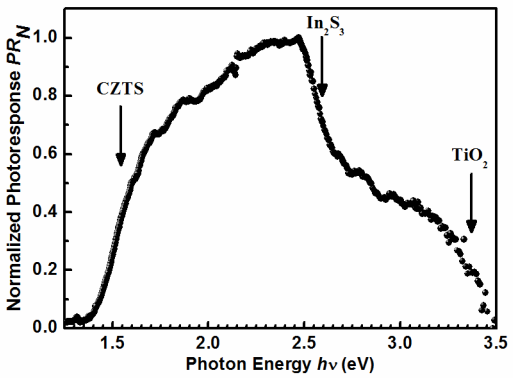

Figure 2: Photoresponse (normalized) against incident photon energy *hν* for the cell FTO/TiO_2/In_2S_3/Cu_2ZnSnS_4/graphite. Vertical arrows indicate the starting point of the main spectral features associated with each layer of the cell.

Figure 2 shows the photoresponse (*PR*), in terms of the normalized spectrum against the incident photon energy *hν* onto CZTS cell. Within the infrared region, the signal is very small (almost zero), showing almost no PR originated in sub-band gap (defect) states [28]. As the photon energy is increased, the PR increases sharply, with a distinct onset of the response and an edge close to 1.5 eV (≈ 800 nm). This edge must be related to the absorption of photons by

CZTS [29]. The PR grows until it reaches a maximum close to 2.45 eV (≈ 500 nm) and then the signal decays abruptly. This decrease could be related to the absorption edge of the In_2S_3 buffer layer, located ca. 2.65 eV [12, 28]. As the absorption of In_2S_3 becomes important less photons will be available for charge carrier generation in the absorber, leading to a lower PR. This suggests that the main charge separation region is between the absorber (CZTS) and the buffer layer (In_2S_3), as expected. Finally, the high energy photons will be absorbed by both the In_2S_3 and the TiO_2 layers and the PR signal will become almost zero in the ultraviolet region.

The optical absorption of the CZTS cell is presented in Figure 3. The inset shows the Incident Photon to electron Conversion Efficiency (IPCE) spectrum obtained from the PR. As the IPCE is proportional to the absorbed photons it can be taken as the absorption coefficient, i. e. a linear region in the $(IPCE * h\nu)^2$ is expected for a direct absorption edge. The extrapolation to zero of the linear fitting gives the position of the direct band gap energy at 1.54 eV, close to the accepted value for CZTS [29-31].

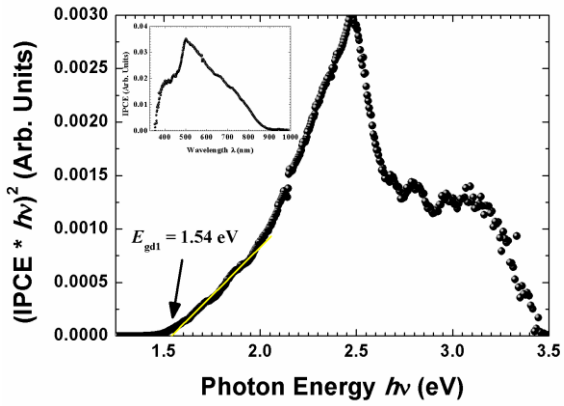

Figure 3: Absorption spectrum for the FTO/TiO_2/In_2S_3/Cu_2ZnSnS_4/graphite cell. Inset: IPCE

4 Conclusions A CZTS solar cell in superstrate configuration FTO/TiO_2/In_2S_3/CZTS/graphite was fabricated entirely by non-vacuum processes and with environmentally friendly compounds. This solar cell displayed excellent performance, with an efficiency of 3.5% which is the highest power conversion efficiency reported for this combination of materials. Electrical and optical parameters were analysed and compared to a similar CIS solar cell, in order to understand the performance of the device. An analysis of the local structure of CZTS that will allow identifying secondary phases, native defects and disorder in the network is in progress.

Acknowledgements The Argentinean authors acknowledge the financial support from (CONICET-ANII MOV_CO_2013_1_ 100005), ANPCyT (PICT 972/15) and Universidad Nacional de Mar del Plata (ING477/16). The Uruguayan authors also acknowledge funding from ANII (Agencia Nacional de Investigación e Innovación) Projects FSE_1_2014_1_102184 and FCE_1_2014_1_104739, CSIC and PEDECIBA – Física, Uruguay.

References

[1] G. Phipps, C. Mikolajczak, T. Guckes, Renewable Energy Focus 9, 56-59 (2008).
[2] S. Siebentritt, Thin Solid Films 535 1-4(2013).
[3] D.B. Mitzi, O. Gunawan, T.K. Todorov, K. Wang, S. Guha, Solar Energy Materials and Solar Cells 95 1421-1436(2011).
[4] W. Ki, H.W. Hillhouse, Advanced Energy Materials 1 732-735(2011).
[5] D.B. Mitzi, O. Gunawan, T.K. Todorov, D.A.R. Barkhouse, Philosophical Transactions of the Royal Society A: Mathematical, Physical and Engineering Sciences 371, 20110432 (2013).
[6] T. Shin, I. Tadayoshi, H. Hirofumi, O. Keiichiro, A. Ryoji, Applied Physics Express 8 082302(2015).
[7] A. Ennaoui, et al., Thin Solid Films 517 2511-2514(2009).
[8] N. Moritake, Y. Fukui, M. Oonuki, K. Tanaka, H. Uchiki, physica status solidi (c) 6 1233-1236(2009).
[9] A. Ghosh, R. Thangavel, A. Gupta, Journal of Alloys and Compounds 694 394-400(2017).
[10] Q. Chen, S. Cheng, S. Zhuang, X. Dou, Thin Solid Films 520, 6256-6261(2012).
[11] R. O'Hayre, M. Nanu, J. Schoonman, A. Goossens, Nanotechnology 18 (2007).
[12] T. Sall, B. Marí Soucase, M. Mollar, B. Hartitti, M. Fahoume, Journal of Physics and Chemistry of Solids 76 100-104(2015).
[13] S.M. Pawar, B.S. Pawar, A.V. Moholkar, D.S. Choi, J.H. Yun, J.H. Moon, S.S. Kolekar, J.H. Kim, Electrochimica Acta 55 4057-4061(2010).
[14] Y.D. Iorio, M. Vázquez, Materials Research Express 4 045903(2017).
[15] P. Panayotatos, H.C. Card, IEE Proceedings I: Solid State and Electron Devices 127 308-311(1980).
[16] K. Masato, T. Kunihiko, M. Katsuhiko, U. Hisao, Japanese Journal of Applied Physics 51 10NC33(2012).
[17] Q.-M. Chen, Z.-Q. Li, Y. Ni, S.-Y. Cheng, X.-M. Dou, Chinese Physics B 21 038401(2012).
[18] Y. Zhang, Y. Sun, H. Wang, H. Yan, physica status solidi (a) 213 1324-1328(2016).
[19] Y. Ren, J.J.S. Scragg, C. Frisk, J.K. Larsen, S.-Y. Li, C. Platzer-Björkman, physica status solidi (a) 212 2889-2896(2015).
[20] N.R. Paudel, K.A. Wieland, A.D. Compaan, Solar Energy Materials and Solar Cells 105 109-112(2012).
[21] R.S.a.H.-W. Schock, Chalcogenide Photovoltaics. Physics, Technologies, and Thin Film Devices, Wiley, 2011.
[22] A. Cazzaniga, et al., Solar Energy Materials and Solar Cells 166 91-99(2017).

[23] L.M. Peter, E.A. Ponomarev, D.J. Fermín, Journal of Electroanalytical Chemistry 427 79-96(1997).
[24] E.A. Ponomarev, L.M. Peter, Journal of Electroanalytical Chemistry 396 219-226(1995).
[25] L. Dloczik, O. Ileperuma, I. Lauermann, L.M. Peter, E.A. Ponomarev, G. Redmond, N.J. Shaw, I. Uhlendorf, The Journal of Physical Chemistry B 101 10281-10289(1997).
[26] G. Schlichthörl, N.G. Park, A.J. Frank, The Journal of Physical Chemistry B 103 782-791(1999).
[27] L. Bertoluzzi, S. Ma, Physical Chemistry Chemical Physics 15 4283-4285(2013).
[28] A.H. Cheshme Khavar, A.R. Mahjoub, H. Fakhri, Journal of Inorganic and Organometallic Polymers and Materials 26 1075-1086(2016).
[29] K.V. Gurav, S.M. Pawar, S.W. Shin, M.P. Suryawanshi, G.L. Agawane, P.S. Patil, J.H. Moon, J.H. Yun, J.H. Kim, Applied Surface Science 283 74-80(2013).
[30] K. Cheng, J. Meng, X. Wang, Y. Huang, J. Liu, M. Xue, Z. Du, Materials Chemistry and Physics 163 24-29(2015).
[31] Y. Li, T. Yuan, L. Jiang, Z. Su, F. Liu, Journal of Alloys and Compounds 610 331-336(2014).